AIP | Journal of Applied Physics

Stimulated crystallization of melt-quenched Ge2Sb2Te5 films employing femtosecond laser double pulses

Rebecca L. Cotton and Jan Siegel

Citation: J. Appl. Phys. **112**, 123520 (2012); doi: 10.1063/1.4770493
View online: http://dx.doi.org/10.1063/1.4770493
View Table of Contents: http://jap.aip.org/resource/1/JAPIAU/v112/i12
Published by the American Institute of Physics.

Additional information on J. Appl. Phys.

Journal Homepage: http://jap.aip.org/
Journal Information: http://jap.aip.org/about/about_the_journal
Top downloads: http://jap.aip.org/features/most_downloaded
Information for Authors: http://jap.aip.org/authors

ADVERTISEMENT

Downloaded 02 Apr 2013 to 161.111.22.141. This article is copyrighted as indicated in the abstract. Reuse of AIP content is subject to the terms at: http://jap.aip.org/about/rights_and_permissions

Stimulated crystallization of melt-quenched $Ge_2Sb_2Te_5$ films employing femtosecond laser double pulses

Rebecca L. Cotton and Jan Siegel[a)]
Laser Processing Group, Instituto de Optica, CSIC, Serrano 121, E-28006 Madrid, Spain

(Received 31 July 2012; accepted 27 November 2012; published online 26 December 2012)

The phase transformation of $Ge_2Sb_2Te_5$ films from the melt-quenched amorphous phase into the crystalline phase induced by 800 nm, 100 fs laser pulses has been studied. For partly amorphized films, progressive crystallization could be induced by single pulses, which can be explained by growth of already existing crystalline embryos. For completely amorphized films, it was not possible to induce crystallization with one or two consecutive pulses; three pulses being the threshold for the onset of crystallization. By employing a fs laser double pulse with an adjustable inter-pulse delay, partial crystallization could be triggered for a delay range of 200 fs–100 ps, while for longer delays no crystallization was possible. The time window for stimulated crystallization can be related to the relaxation dynamics of free electrons excited by the first pulse, which are further excited by the second pulse still remaining in the excited state. Our results indicate that the lifetime of excited electrons in melt-quenched amorphous $Ge_2Sb_2Te_5$ is ≈100 ps. © *2012 American Institute of Physics*. [http://dx.doi.org/10.1063/1.4770493]

I. INTRODUCTION

Optical recording in chalcogenide films is an established technology for storage of binary information on phase change optical disks (PCODs), such as rewritable CDs, DVDs, and Blu-ray disks.[1] Its concept is based on laser pulse-induced switching between the amorphous and crystalline phases of the films. Data read-out is done also optically, exploiting the fact that the crystalline and amorphous phases have different reflectivities.[2] Despite the remarkable performance of state-of-the-art products, the data transfer rate is limited by the duration of the laser pulses used, which is a few tens of nanoseconds (ns) for triggering phase transitions.[3]

The use of ultrashort laser pulses, currently available only at laboratory level, for performing switching operations would allow surpassing current benchmarks by several orders of magnitude. The proof-of-concept of ultrafast reversible phase switching has been done already in the nineties in GeSb films using picosecond (ps) and femtosecond (fs) pulses.[4–7] In $Ge_2Sb_2Te_5$, which is the standard composition used in most PCODs, reversible phase change has been demonstrated somewhat later for single ps pulses,[8,9] whereas crystallization of the as-grown amorphous phase was also achieved with single fs pulses.[10] In a related composition within the GeTe-Sb_2Te_3 pseudo-binary system, $Ge_1Sb_4Te_7$, both amorphization and crystallization has been achieved using single sub-ps laser pulses.[11]

However, only in some of these works[8,9] the dynamics of the phase transitions were studied in order to shed light on the underlying mechanisms. In this context, it is important to remark that the amorphization process is straight-forward to trigger with ultrashort laser pulses in phase-change materials since it normally requires ultrafast melting and quenching, which is inherent to the use of ultrashort pulses.[7] Recent studies provide evidence that there is an alternative pathway for amorphization, without passing through the molten phase, in form of a photo-assisted process generating sufficiently high carrier densities to trigger the phase transition.[12,13]

In contrast, crystallization is more problematic to achieve with ultrashort pulses, due to the existence of a minimum time required for stable crystalline nuclei to form and grow. A number of parameters have been identified and adjusted in order to favor crystallization with ultrashort pulses, including thermal heat flow conditions defined by the film-substrate system,[8] doping[14] or vacancies.[15] Recently, the use of a closely spaced double pulse sequence has been proposed Makino *et al.*[16] in order to trigger crystallization in chalcogenide films via coherent excitation of optical phonons. The authors study a phase transition in amorphous GeTe/Sb_2Te_3 superlattices (GST-SLs), whose added composition is that of $Ge_2Sb_2Te_5$. Employing coherent phonon spectroscopy based on a pump-probe scheme using a high repetition rate laser with a pulse width of 20 fs, the authors provide clear evidence for a phase transition induced by double pulse pairs with a well-defined pulse separation (276 fs). Due to the lack of a pulse picker in their experimental setup, the authors could not yet investigate if a single pulse pair is sufficient to trigger crystallization. It is worth emphasizing though, that the achievement of phase switching in GST-SL via excitation of coherent phonons does not imply that the same strategy would work in non-layered $Ge_2Sb_2Te_5$ films. GST-SL are significantly more structured, which manifests by requiring a factor of ten lower pulse energy for phase switching than equivalent GST films.

The aim of this work is to apply the concept of double pulse excitation to stimulate the amorphous-crystalline phase transition in conventional $Ge_2Sb_2Te_5$ films. In contrast to the work reported in Ref. 16, we do not employ coherent phonon spectroscopy to monitor frequency shifts of the phonon modes

[a)]Author to whom correspondence should be addressed. Electronic mail: j.siegel@io.cfmac.csic.es.

 © 2012 American Institute of Physics

Downloaded 02 Apr 2013 to 161.111.22.141. This article is copyrighted as indicated in the abstract. Reuse of AIP content is subject to the terms at: http://jap.aip.org/about/rights_and_permissions

but rely on an increase of the steady state-reflectivity, which is indicative of crystallization. This approach allows us to perform our experiment in a non-repetitive, single exposure mode, thus ensuring that crystal growth of nuclei formed in a previous exposure is not influencing the experimental results.

II. EXPERIMENTAL CONFIGURATION

The laser used was a regenerative Ti:Sa amplifier operating at 800 nm wavelength with a pulse duration of 100 fs. Single pulses were picked from the 100 Hz pulse train by means of an electromechanical shutter. The setup for stimulated crystallization with temporally delayed double pulses, displayed in Fig. 1, consists of two pump beams P1 and P2, with P1 being incident at 53° and P2 at 0°. P1 is apertured down to a diameter of 2 mm and focused by means of a convex lens ($f = +150$ mm) onto the sample surface to an elliptical spot size 180 μm × 112 μm ($1/e^2$—intensity diameters). The intensity distribution at the sample surface has been determined to be Gaussian, thus providing a well-defined relation between local fluence and position with respect to the spot center.[17] P2 is sent through a concave lens ($f = -500$ mm) before entering a long working distance objective lens (N.A. = 0.40), which focuses it at the sample surface. The presence of the concave lens avoids strong focusing of P2, yielding an approximately circular spot size of 24 μm ($1/e^2$—intensity diameter), whose intensity distribution is Gaussian only to a very limited extent. Besides focusing P2, the second purpose of the objective lens is to form an image of the sample surface on the chip of a charge coupled device (CCD) camera, in combination with a tube lens ($f = 200$ mm). Wide-field illumination of the sample surface is achieved by employing a light emitting diode (LED) at 400 nm.

The sample used was a 40 nm thick, fcc crystalline $Ge_2Sb_2Te_5$ film on top of a 100 nm thick SiO_2 buffer layer on a silicon wafer. Since the double pulse experiment requires the sample to be in a melt-quenched state, the $Ge_2Sb_2Te_5$ film was locally amorphized by exposure to a single fs laser pulse of P1. In a previous work, we have studied the amorphization of these films upon irradiation with a single fs laser using optical fs microscopy.[17] We have obtained results which are fully consistent with melting and subsequent amorphization via quenching. In order to obtain complete amorphization within the central region of the spot, a series of irradiations at different fluences was performed. Since amorphization is accompanied by a strong decrease of the film reflectivity, the evaluation of the irradiation study could be followed and quantified by means of the *in situ* microscope. The result yielded an optimum fluence of $F_{P1} = 53$ mJ/cm^2 for complete amorphization with P1, the corresponding optical micrograph and reflectivity profile being shown in Fig. 2. The micrograph shows a pronounced dark elliptical disk, indicative of amorphization. The light grey ring and the darkest ring have been identified as regions with different degrees of (incomplete) amorphization, whereas the central disk, slightly brighter than the darkest ring corresponds to complete amorphization.[17] As can be seen in the reflectivity profile, different degrees of amorphization are accompanied by a continuous change in reflectivity decreasing down to $R = 0.77$, whereas full amorphization leads to a reflectivity recovery up to $R = 0.82$, which is consistent with calculations using the optical properties of the two phases and the film thickness.[17]

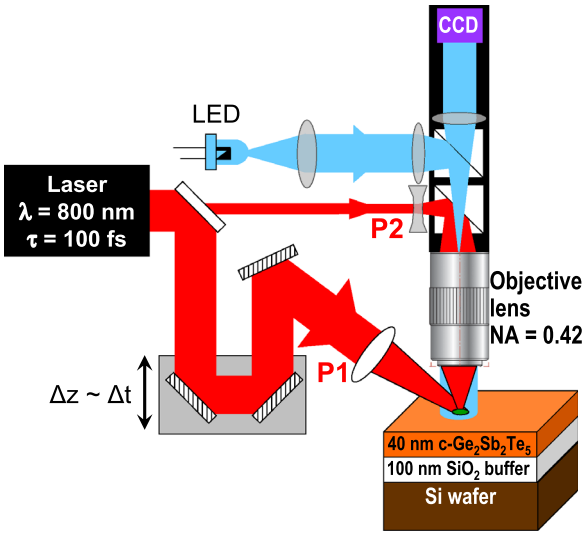

FIG. 1. Setup for performing the experiment of stimulated crystallization with temporally delayed double pulses. Laser beams P1 and P2 are derived from the same laser and delayed via an optical delay line, incident at different angles and spatially overlapped at the sample surface.

III. RESULTS AND DISCUSSION

A. Determining the threshold fluence and pulse number for crystallization

As a first step, it is crucial to investigate if a fluence range exists in our particular film/substrate system for a single fs laser pulse to trigger crystallization of the melt-quenched amorphous film. We have performed a systematic study,

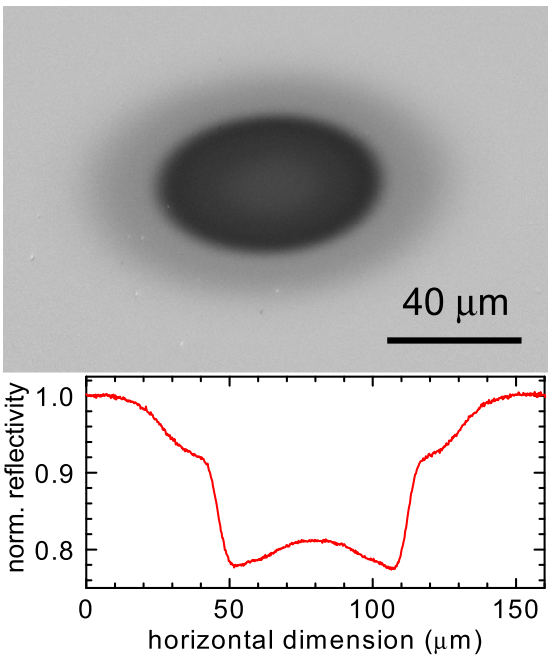

FIG. 2. *In situ* micrograph of a melt-quenched amorphous region of the sample (top) using P1, together with the corresponding reflectivity profile along the horizontal axis (bottom). The reflectivity has been normalized to the one of the unexposed crystalline region.

Downloaded 02 Apr 2013 to 161.111.22.141. This article is copyrighted as indicated in the abstract. Reuse of AIP content is subject to the terms at: http://jap.aip.org/about/rights_and_permissions

irradiating a series of melt-quenched regions with single pulses of P2 with increasing energies. In no case, a reflectivity increase (indicative of crystallization) could be observed. In this context, it is worth emphasizing that our study is performed on a melt-quenched amorphous phase. Several authors have reported that the crystallization rate from such a state is higher than from an as-grown state.[18,19] We find that crystallization with single fs laser pulses of a melt-quenched state is not possible in our case. We believe that the reason for this behaviour is that a melt-quenched state produced by a fs laser pulse (as in our case) is considerably more pure amorphous than that produced by a ns laser pulse as used in Refs. 18 and 19, which tend to produce an amorphous phase with remaining crystalline embryos, due to the lower cooling rate achieved. There is, however, one work published that we are aware of, which reports crystallization from the as-grown state by fs laser pulses.[10] The authors observe an increase in grain size upon fluence increase, which they attribute to the larger melt depth and release of latent heat, thus lowering the cooling rate. The important difference to our situation is the substrate their film is supported on, being carbon with a low thermal diffusivity and thus favouring crystallization. In contrast the substrate of our film is silicon, ensuring very fast heat extraction and thus favouring amorphization. It is worth noting that a recent work reports re-crystallization from a melt-quenched state back into the initial epitaxial state by not more than ten femtosecond laser pulses at low fluence.[20] The authors attribute this astonishing ability to either a latent memory of the amorphous phase of its original state or the single crystalline interface being crucial for nucleation and growth.

While measurable crystallization of the melt-quenched amorphous region is not possible with a single pulse, it can be achieved by irradiation with multiple fs laser pulses, typically many tens.[17] We have performed a systematic study, irradiating a series of melt-quenched regions with 200 pulses of P2 at different peak fluences, evaluating the degree of crystallization as a function of fluence. We observed an almost complete recovery of the reflectivity of the crystalline material (full crystallization) at a fluence of $F_{P2} = 17$ mJ/cm^2. We have chosen this fluence to perform a study of the reflectivity increase as a function of pulse number.

Fig. 3 shows the results of a study in which the amorphous spot has been irradiated in the center with P2 at the selected fluence $F_{P2} = 17$ mJ/cm^2. Because of the weak reflectivity change at low pulse numbers, image normalization had to be done with respect to the pre-amorphized spot and not with respect to the unexposed film. In that way, the weak reflectivity recovery is not masked by the strong contrast of the amorphized spot and can be appreciated over a constant background. Fig. 3(a) shows the melt-quenched film after irradiation with two consecutive single pulses of P2. The absence of a reflectivity increase in the center demonstrates that neither one nor two pulses are able to induce partial crystallization. In fact, a careful analysis showed that one and two pulses trigger a weak reflectivity decrease. In contrast, for three pulses (Fig. 3(b)) a reflectivity increase was observed. The micrographs for 5 pulses (Fig. 3(c)) and more (Fig. 3(d)) show a marked reflectivity increase. The signs of

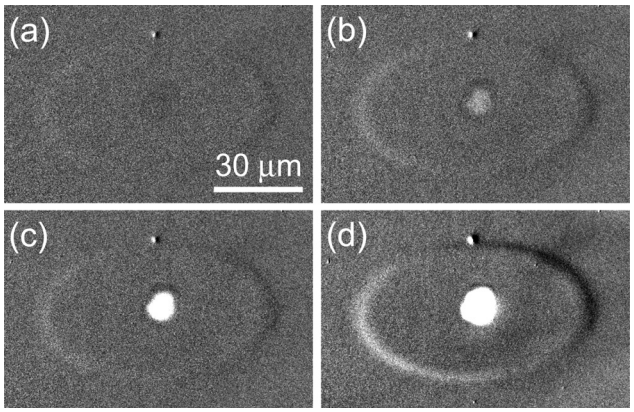

FIG. 3. *In situ* micrographs of the same melt-quenched region of the sample upon irradiation of the central region with (a) two, (b) three, (c) five, and (d) ten laser pulses of P2. The micrographs have been normalized to the micrograph of the amorphous spot, in order the reveal the weak effect of P2, inducing a reflectivity change in the central region.

image saturation in these micrographs are caused by choosing a narrow look up table and fixing it to be the same for all images. In that way, progressive crystallisation manifests mainly by apparent lateral growth of the crystallized region.

While the micrographs displayed in Fig. 3 were scaled to improve contrast and thus suffer from saturation, the raw data acquired was not saturated in order to perform quantitative data analysis. For each micrograph, a horizontal profile through the spot center was extracted and analyzed as shown in the inset of Fig. 4 for the case of 10 pulses. The main frame of Fig. 4 represents the peak reflectivity value in the center of the recrystallized region as a function of number of pulses. As can be seen, the peak reflectivity increases strongly with pulse number up to ≈ 10 pulses. After that the reflectivity begins to saturate and then decreases significantly, possibly due to film degradation caused by selective evaporation and/or oxidation.[21] Consistently with the results of Fig. 3, the threshold for reflectivity increase in Fig. 4 is three pulses, which confirms the existence of two incubation pulses before re-crystallization sets in, triggered by a third pulse.

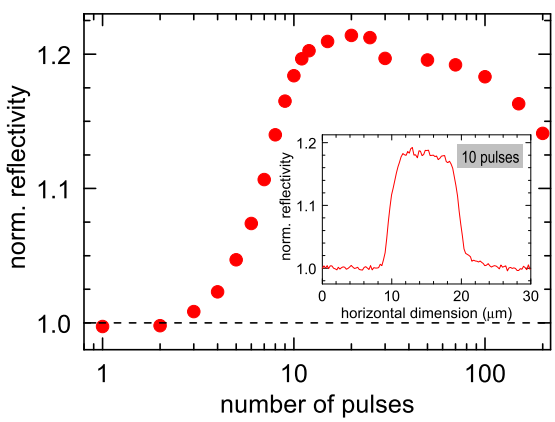

FIG. 4. Evolution of the reflectivity in the central region of a melt-quenched region as a function of pulse number of P2. The reflectivity has been normalized to the micrograph of the amorphous spot. Any increase above unity corresponds therefore to (partial) crystallization, which occurs at three pulses. The inset shows the reflectivity profile along the horizontal axis of a spot irradiated by 10 pulses.

Downloaded 02 Apr 2013 to 161.111.22.141. This article is copyrighted as indicated in the abstract. Reuse of AIP content is subject to the terms at: http://jap.aip.org/about/rights_and_permissions

B. Crystallization using sub-threshold double pulses with adjustable inter-pulse delay

For the following study, we have set the fluence of P1 to an sub-threshold value of $F_{P1} = 25\,mJ/cm^2$, equivalent in terms of absorbed energy to $F_{P2} = 17\,mJ/cm^2$ in order to perform double pulse irradiation with temporally delayed pulses of equal absorbed fluence, below the crystallization threshold.[22] Using an optical delay line, P2 is delayed with respect to the arrival of P1, which enables us to explore a wide range of temporal delays between both pulses. Representative results are displayed in Fig. 5. The *in situ* micrographs, recorded after double pulse irradiation, illustrate two different phenomena. First, a common, delay-independent annular reflectivity increase at the spot border (bright elliptical rings in Figs. 5(a)–5(d)), which lies outside the overlap region of P1 and P2. This increase can be attributed to a progressive crystallization of a region that is a mixture of amorphous and crystalline (corresponding to the weak grey ring in Fig. 2) caused by P1 alone. This progressive crystallization is indicative of growth-dominated crystallization originating from pre-existing crystalline material at the border of the amorphous spot.

Second, a delay-dependent reflectivity change in the overlap region of P1 and P2 (dashed circles in Fig. 5). For zero delay (Fig. 5(a), a marked and somehow irregular reflectivity decrease can be observed in the overlap region, which we identify as film ablation. Excitation with two temporally and spatially coincident pulses causes higher instantaneous energy deposition compared to excitation with two non-delayed pulses (such as displayed in Fig. 3(a)). It is worth noting that under these conditions, we also observe a pattern of vertical fringes (see inset in Fig. 5(a)) in the overlap region, due to optical interference of P1 and P2. We have measured its period with a high-resolution optical microscope to be $p_{exp} \approx 880$ nm, which is consistent with the theoretical value $p_{theo} = 896$ nm expected for two beam interference ($p_{theo} = \lambda/(2*\sin(\theta/2))$). For a delay of 300 fs (Fig. 5(b)), no interference fringes are observed and the overlap region shows a slightly enhanced reflectivity, compared to the unexposed region, which is indicative of partial crystallization. In contrast, for much longer delays such as 500 ps or 1 s (Figs. 5(c) and 5(d), respectively), the reflectivity in the overlap region is the same as, or below the one in the unexposed region.

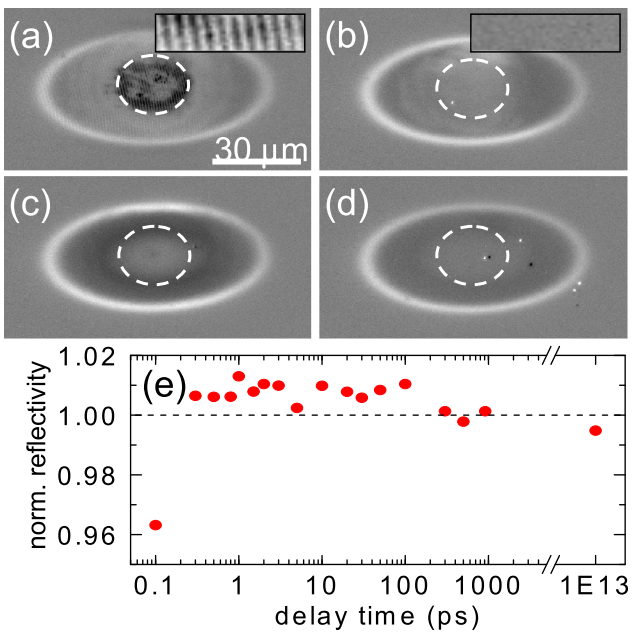

FIG. 5. *In situ* micrographs of a melt-quenched region upon irradiation of the central region with temporally delayed fs laser pulses. P2 is delayed with respect to P1 by (a) 0 ps, i.e., temporally coincident, (b) 0.3 ps, (c) 500 ps, and (d) 1 s. The overlap region of P1 and P2 is marked by a dashed circle, showing the spatial extension ($1/e^2$ diameter) of P2. The insets in (a) and (b) are 10 μm × 3 μm magnifications of the center region to reveal the presence or absence interference effects in the corresponding micrographs. The micrographs have been normalized to the micrograph of the amorphous spot. The graph at the bottom shows the evolution of the reflectivity in the very center of a melt-quenched region upon irradiation with temporally delayed fs laser pulses as a function of delay time.

We have recorded and analyzed a series of micrographs, averaging the normalized reflectivity in the very center of the overlap region, over an area of about 5 μm in diameter. Fig. 5(c) represents the reflectivity evolution as a function of delay time. It can be seen that for a broad range of delays (200 fs–100 ps) the normalized reflectivity increases above unity. For longer delays, no reflectivity increase can be observed. This demonstrates stimulated crystallization by temporally delayed fs pulses for a limited inter-pulse delay range. This conclusion points to a mechanism being responsible for the crystallization process, whose lifetime is in the order of $\tau \approx 100$ ps. The fact that the mechanism is ultrafast (onset at 200 fs) excludes a thermal origin. The generation of free electrons is the most probable reason, which is expected to be very efficient in amorphous $Ge_2Sb_2Te_5$, which has a small band gap (0.7 eV)[27] and thus allows linear absorption of the laser light (1.55 eV), generating free electrons in the conduction band. In this scenario, the electron density increases strongly upon irradiation with P1 and decays within approximately 100 ps. If P2 arrives later than this delay, it excites the film in a relaxed state with a low number of free electrons. P2 therefore triggers a similar increase in electron density as P1, which also relaxes after another 100 ps. In this situation, the final reflectivity change induced in the material is below unity and comparable to the one of temporally uncorrelated pulses P1 and P2 (Fig. 5(d)) or two incubation pulses (Fig. 4). However, if P2 arrives before the excited electrons have relaxed, it further excites the material, thus triggering the onset of crystallization. The effect of temporally delayed double pulses on the crystallization behaviour in comparison to the effect of uncorrelated pulses or single pulses is represented in Fig. 6. Shown is the case of best re-crystallization, which is obtained for a delay of 1 ps, yielding a reflectivity increase of 1.1%. While this may appear small, it is still significant, reproducible and not achievable with uncorrelated pulses.

As for the free electron lifetime value extracted from our experiment ($\tau \approx 100$ ps), we can compare our results to those reported by Zhang and co-workers.[23] The authors study the electron relaxation dynamics in amorphous $Ge_2Sb_2Te_5$ using a pump-probe technique upon excitation with a 130 fs laser pulse at 400 nm and fluences up to $11\,mJ/cm^2$. They observe two decay components; a fast decay within a few ps and a slow decay within 1 ns. They attribute the fast decay to

Downloaded 02 Apr 2013 to 161.111.22.141. This article is copyrighted as indicated in the abstract. Reuse of AIP content is subject to the terms at: http://jap.aip.org/about/rights_and_permissions

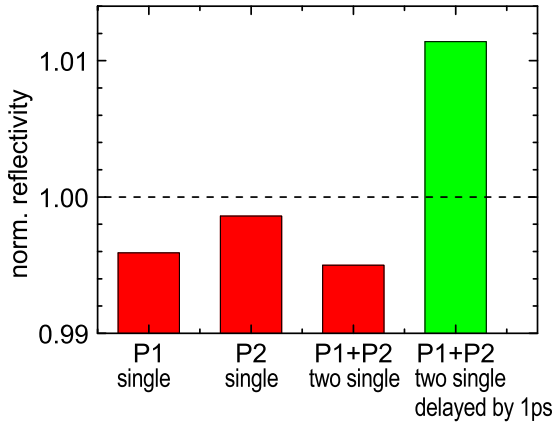

FIG. 6. Reflectivity change in the center of the melt-quenched region induced upon irradiation of amorphous spots by sub-threshold pulses: P1 only, P2 only, P1 and P2 temporally separated by 1 s, and P1 and P2 with a delay time of 1 ps. The reflectivity is normalized to the one of an amorphous spot.

intraband carrier relaxation and carrier trapping, whereas the slow decay is interpreted as due to recombination of trapped carriers. One has to keep in mind that those results were obtained in as-grown amorphous material, as opposed to our conditions of melt-quenched amorphous material. Many studies have provided evidence of important differences in the crystallization behaviour[18,19] and the amorphous structure[24,25] of melt-quenched and as-grown films. We therefore interpret our measured lifetime value ($\tau \approx 100$ ps) as an effective carrier lifetime in fs-laser melt-quenched $Ge_2Sb_2Te_5$ films at relatively high fluences ($F_{P2} = 17$ mJ/cm^2). The free electron density can be estimated in our conditions according to the equation[26] $N_e = [(1-R(0°))*\alpha*F_{P2}]/[\hbar\omega_0]$, with $R(0°) \approx 0.46$, the absorption coefficient[27] $\alpha = 2.2 \times 10^5$ cm^{-1} and $\hbar\omega_0 = 1.55$ eV. The value obtained is $N_e = 8.1 \times 10^{21}$ cm^{-3}, a factor of 2.5 higher than reported in Ref. 23. This high electron density in combination with our double pulse excitation approach is the likely origin of the stimulated crystallization we observe.

IV. CONCLUSIONS

We have studied the crystallization behaviour of melt-quenched amorphous $Ge_2Sb_2Te_5$ films upon irradiation with femtosecond laser pulses. Melt-quenched amorphous regions were produced by exposure to a single laser pulse and characterized by *in situ* microscopy according to their reflectivity level. Using irradiation with single laser pulses of varying fluence it was verified that for our sample (40 nm thick, 100 nm SiO_2 buffer layer on Si substrate) crystallization was not possible, requiring a minimum pulse number of three for triggering partial crystallization. In contrast, it was possible to trigger partial crystallization by irradiating with a double pulse, provided that the inter-pulse delay was in the range of 200 fs–100 ps. At zero delay we observed ablation, due to the local intensity enhancement of interfering pulses. At delays larger than 100 ps, no crystallization was induced. We conclude that the maximum delay for stimulated crystallization (100 ps) is a direct measure of the lifetime of the free electrons excited by the first pulse, which are further excited by the second pulse while still being in the excited state. For conditions where melt-quenching produced only partly amorphized films, progressive crystallization by single pulses was observed (without the need of temporally delayed pulses), which can be explained by growth of the already existing crystalline phase.

ACKNOWLEDGMENTS

The authors thank E. Varesi, A. Pirovano, and R. Bez from Numonyx, Agrate Brianza, Italy for supplying the GST films. This work has been partially supported by the EU projects CHEMAPH (IST-027561) and by the Spanish Ministry of Science and Innovation (TEC2008-01183).

[1]A good overview of the background, technology and different generations of the optical disks and its different format can be found at http://en.wikipedia.org/wiki/Optical_disc.
[2]S. R. Ovshinsky, Phys. Rev. Lett. **21**, 1450 (1968).
[3]N. Yamada, E. Ohno, K. Nishiuchi, N. Akahira, and M. Takao, J. Appl. Phys. **69**, 2849 (1991).
[4]C. N. Afonso, J. Solis, F. Catalina, and C. Kalpouzos, Appl. Phys. Lett. **60**, 3123 (1992).
[5]M. C. Morilla, J. Solis, and C. N. Afonso, Jpn. J. Appl. Phys., Part 1 **36**, 1015 (1997).
[6]J. Siegel, C. N. Afonso, and J. Solis, Appl. Phys. Lett. **75**, 3102 (1999).
[7]T. Ohta, N. Yamada, H. Yamamoto, T. Mitsuyu, T. Kozaki, J. Qiu, and K. Hirao, Mater. Res. Soc. Symp. Proc. **674**, V1.1.1 (2001); T. Ohta, J. Optoelectron Adv. Mater. **3**, 609 (2001); T. Ohta and N. Yamada, in Proceedings of E/PCOS, Säntis, Switzerland, 2001, http://www.epcos.org/papers/pdf_2001/Ohta.pdf.
[8]J. Siegel, A. Schropp, J. Solis, C. N. Afonso, and M. Wuttig, Appl. Phys. Lett. **84**, 2250 (2004).
[9]H. Huang, F. Zuo, F. Zhai, Y. Wang, T. Lai, Y. Wu, and F. Gan, J. Appl. Phys. **106**, 063501 (2009).
[10]G. Zhang, D. Gu, X. Jiang, Q. Chen, and F. Gan, Solid State Commun. **133**, 209 (2005).
[11]S. Y. Huang, Z. J. Zhao, and Z. Sun, Appl. Phys. A **82**, 529–533 (2006).
[12]P. Fons, H. Osawa, A. V. Kolobov, T. Fukaya, M. Suzuki, T. Uruga, N. Kawamura, H. Tanida, and J. Tominaga, Phys. Rev. B **82**, 041203 (2010).
[13]X. B. Li, X. Q. Liu, X. Liu, D. Han, Z. Zhang, X. D. Han, H. B. Sun, and S. B. Zhang, Phys. Rev. Lett. **107**, 015501 (2011).
[14]T.-Y. Lee, K.-B. Kim, B.-K. Cheong, T. S. Lee, S. J. Park, K. S. Lee, W. M. Kim, and S. G. Kim, Appl. Phys. Lett. **80**, 3313 (2002).
[15]M. Wuttig, D. Lüsebrink, D. Wamwangi, W. Wełnic, M. Gille*β*en, and R. Dronskowski, Nat. Mater. **6**, 122 (2007).
[16]K. Makino, J. Tominaga, and M. Hase, Opt. Exp. **19**, 1260 (2011).
[17]J. Siegel, W. Gawelda, D. Puerto, C. Dorronsoro, J. Solis, C. Afonso, J. C. G. de Sande, R. Bez, A. Pirovano, and C. Wiemer, J. Appl. Phys. **103**, 023516 (2008).
[18]P. K. Khulbe, E. M. Wright, and M. Mansuripur, J. Appl. Phys. **88**, 3926 (2000).
[19]R. M. Shelby and S. Raoux, J. Appl. Phys. **105**, 104902 (2009).
[20]P. Rodenbach, A. Giussani, K. Perumal, M. Hanke, M. Dubslaff, H. Riechert, R. Calarco, M. Burghammer, A. V. Kolobov, and P. Fons, Appl. Phys. Lett. **101**, 061903 (2012).
[21]B.-S. Lee and S. G. Bishop, Optical and electrical properties of phase change materials, in *Phase Change Materials*, edited by S. Raoux and M. Wuttig (Springer 2008), Chap. 9.
[22]The elevated angle of incidence of P1 (53°) leads to a decrease of the absorbed energy by a certain factor due to a higher Fresnel reflectivity. For the sample at 800 nm wavelength, this factor can be estimated as $[(1-Rs(0°))]/[(1-Rs(53°))] = 1.53$.
[23]G. Zhang, F. Gan, S. Lysenko, and H. Liu, J. Appl. Phys. **101**, 033127 (2007).
[24]J. Akola, J. Larrucea, and R. O. Jones, Phys. Rev. B **83**, 094113 (2011).
[25]M. Naito, M. Ishimaru, Y. Hirotsu, R. Kojima, and N. Yamada, J. Appl. Phys. **107**, 103507 (2010).
[26]K. Sokolowski-Tinten, J. Bialkowski, and D. von der Linde, Phys. Rev. B **51**, 14186 (1995).
[27]B.-S. Lee, J. R. Abelson, S. G. Bishop, D. H. Kang, B. Cheong, and K. B. Kim, J. Appl. Phys. **97**, 093509 (2005).

Downloaded 02 Apr 2013 to 161.111.22.141. This article is copyrighted as indicated in the abstract. Reuse of AIP content is subject to the terms at: http://jap.aip.org/about/rights_and_permissions